Crack Initiation of Natural Rubber Under High Temperature Fatigue Loading

Gengsheng Weng, Guangsu Huang, Hangxin Lei, Liangliang Qu, Peng Zhang, Yijing Nie, Jingrong Wu

State Key Laboratory of Polymer Material Engineering, College of Polymer Science and Engineering, Sichuan University, Chengdu 610065, People's Republic of China

Received 22 January 2011; accepted 2 August 2011
DOI 10.1002/app.35408
Published online 29 November 2011 in Wiley Online Library (wileyonlinelibrary.com).

ABSTRACT: Vulcanized natural rubber (NR) under quiescent thermal oxidation aging and high temperature fatigue loading with small strain amplitude was investigated by the infrared spectroscopy, scanning electron microscopy, and positron annihilation lifetime spectroscopy measurements. IR results demonstrated the thermal oxidation degradation process of vulcanized NR at 85°C. During high temperature fatigue loading, nanoscale cracks and voids that are generated by the combined impact of thermal oxidation and cyclic loading were detected. Further investigation suggests that the nucleation effect of dissolved vapor and gas in the low molecular weight domains of the NR under fatigue loading accounts for the appearance of nanocracks. This work provides some new insight into the crack initiation mechanism of NR during high temperature fatigue loading, which has not been clearly understood.
 J Appl Polym Sci 124: 4274–4280, 2012

Key words: natural rubber; crack initiation; thermal oxidation aging; high temperature fatigue

INTRODUCTION

Fatigue characteristic of rubbery materials is an important factor that determines the strength and durability of the materials.[1,2] Usually, one is interested in increasing the life of rubbers under fatigue loading. For that, the first step is the description of crack initiation. Most of the studies on the fatigue of elastomers were based on the pure mechanical theories that did not take into account the physical mechanism of crack initiation involved during the fatigue loading.[2–6]

Natural rubber (NR) has been recognized as an indispensable commercial rubber material in many applications such as heavy-duty tires, essential components of vibration isolation structure against earthquakes and medical products, because of its high elasticity, tensile strength, and excellent crack growth resistance.[7–9] Crack initiation in NR at room temperature is described by Le Cam et al.[10] By using scanning electron microscopy (SEM), they propose that cavitation of NR at room temperature takes place around zinc oxide particles at the poles of metallic oxide inclusions, due to the decohesion between oxides and rubber matrix. However, this investigation did not consider the influence of temperature. In most of the applications of NR, heat generated from cyclic deformations at sufficient amplitude and frequency cannot be easily conducted, resulting in the temperature increasing of rubber components.[11–13] It is known that rubber material failure originates from the microscopic crack initiation and its growth. Since, suppression on the crack initiation can increase service life substantially and effectively, research on the crack initiation mechanism is important. Up to now, studies on the crack initiation, physical mechanism of NR under high temperature, and fatigue loading are rarely achieved. High temperatures lead to the thermal degradation of NR vulcanizates. Thus, the crack initiation mechanism may be different.

The positron annihilation lifetime spectroscopy (PALS) measurement gives direct information about the dimension, size distribution, and content of free volume in polymer matrix. There has been several researches reported the relation between free volume and amorphous metallic glass fatigue.[14–16] However, present researches rarely applied the PALS measurement to study the rubber fatigue performance. Recently, Rozanski et al. investigated the effect of stabilizers, additives, and low molecular weight component on the cavitation of polypropylene.[17] On the basis of the PALS measurement, they declared

Correspondence to: G. Huang (guangsu-huang@hotmail.com).

Contract grant sponsor: Major State Basic Research Projects of China; contract grant number: 50673059.
Contract grant sponsor: National Nature Science Foundation of China; contract grant number: 50103007.

TABLE I
Recipes of the Vulcanized NR

Ingredients	Loading level (phr)[a]
NR	100
ZnO	5
Stearic acid	1
Accerlerater CBS[b]	1
Sulfur	2
Curing time (min)	12

[a] Parts by weight per hundred parts rubber (phr).
[b] *N*-Cyclohexyl-2-benzothiazole sulfonamide.

that cavitation is strongly dependent on the free-volume of polypropylene. Inspired by the researches referred above, we used the PALS method to investigate the crack initiation of NR under high temperature fatigue loading.

In this work, we first detected the thermal oxidation degradation of vulcanized NR under quiescent aging by Fourier transform infrared spectroscopy (FTIR). Then, vulcanized NR was subject to high temperature fatigue with small cyclic amplitude (exclude the influence of strain induced crystallization). According to the combined research of SEM and PALS measurements, we finally proposed the crack initiation mechanism of NR under high temperature fatigue loading.

EXPERIMENTAL

NR used in this study was ribbed smoked sheet No. 1 from Indonesia. Nonvulcanized NR, containing all the vulcanization ingredients, was prepared in a laboratory twin roll mixing mill (SK-160B, made by Shanghai Rubber Machine, China) at room temperature, and then vulcanized at 140°C for 12 min under a pressure of 1.5×10^7 Pa. The recipes are shown in Table I.

Mechanical performance of aged NR was tested by an Instron 5567 material testing machine. The tensile specimens were dumbbell-shaped thin strip ($25 \times 6 \times 2$ mm^3) and experiments were performed at a tensile speed of 500 mm min^{-1}. The tear strength was determined according to GB/T529-1999. The test pieces were cut by a right-angle-type cutter. Five samples of each group (different aging time) were tested for statistical accuracy.

Vulcanized NR film with a thickness of about 80 μm was clamped between two metal sheets (sample card). A schematic picture of the homemade sample card was shown in Figure 1. The sample card can directly slide into the slots in the sample holder of the Thermo Nicolet IS 10 spectrometer for transmission analysis. The clamped NR film was exposed in air at 85°C in ventilated oven and removed from oven in every 24 h (totally aged for 8 days) for FTIR analysis. During the whole process, the detecting point of the NR film is not changed.

Dumbbell-shaped rubber specimens ($25 \times 6 \times 2$ mm^3) were subject to cyclic tensile loading using MTS 810 material test machine at a temperature of 85°C. The frequency of loading is 5 Hz and the strain amplitude is 0.5. Because of the small strain amplitude, strain induced crystallization does not occur.[18] The testing procedures for each sample were terminated at definite times. Finally, eight samples with different fatigue times were obtained. Corresponding cyclic tensile loading at room temperature were also achieved under the same condition.

The morphology of the samples was studied by SEM. The samples first cryogenically fractured in liquid nitrogen. Then, the fractured surface was coated with a thin layer of gold. Finally, the samples were observed and investigated by a SEM instrument (Inspect F, FEI company) operation at 20 kV.

A 30 μCi 22Na positron source sealed between two sheets of nickel foil (1 mg/cm^2) was sandwiched between two pieces of the samples. Positron lifetime spectra were measured using a conventional fast–fast coincidence spectrometer. The time resolution of the system was found to be a sum of two Gaussian curves with full width of half maximum (FWHM) =280 ps (90%) and 320 ps (10%). The obtained positron lifetime spectra were resolved into three components employing the PATFIT program after the background and positron source correction were subtracted. The shortest lifetime (τ_1) is the lifetime of the singlet-positron (p-Ps) and the intermediate lifetime (τ_2) is the lifetime of the positron. The longest lifetime (τ_3) is due to the orthopositronium (o-Ps) pickoff annihilation in the free volume holes in the amorphous phase. Considering that only the o-Ps component is significantly sensitive to the change in the microstructure of the amorphous phase, the results of o-Ps lifetime were employed to obtain the mean free volume parameters.

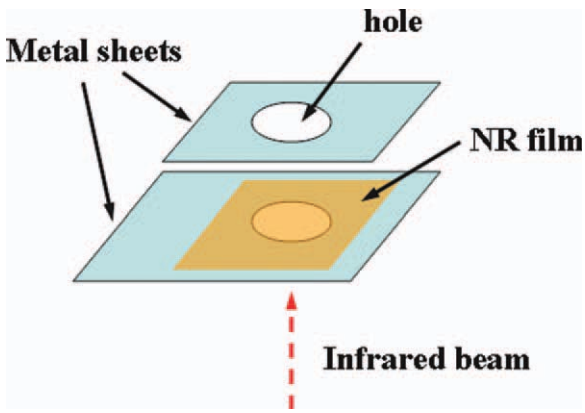

Figure 1 Schematic representation of the homemade sample card. [Color figure can be viewed in the online issue, which is available at wileyonlinelibrary.com.]

TABLE II
Properties Variation of the Vulcanized NR under Thermal Oxidation Aging

Time (day)	Tear strength (KN/m)	Modulus at 100% elongation (MPa)	Tensile strength (MPa)	Elongation at break (%)
0	53 ± 2	0.85 ± 0.03	17.5 ± 0.2	670 ± 10
1	52 ± 3	0.84 ± 0.04	17.6 ± 0.4	665 ± 8
2	51 ± 1	0.79 ± 0.02	16.2 ± 0.2	650 ± 10
3	50 ± 4	0.68 ± 0.01	16.4 ± 0.3	628 ± 5
4	49 ± 3	0.65 ± 0.03	13.8 ± 0.5	619 ± 10
8	47 ± 2	0.57 ± 0.02	10.1 ± 0.4	552 ± 7

RESULTS AND DISCUSSION

Mechanical properties variation of the NR under thermal oxidation aging at typical aging times is shown in Table II. Obviously, tear strength, modulus at 100% elongation, tensile strength, and elongation at break of NR decreases gradually when subject to thermal oxidation aging. Similar mechanical performance results can be seen in the previous studies.[19] The deterioration of mechanical properties is resulted from the NR microstructure destruction. To understand the thermal oxidation aging process, FTIR measurements were employed. Figure 2(a) shows the time independence of the FTIR spectra of the vulcanized NR at an aging temperature of 85°C. All the usual peaks are presented for *cis*-polyisoprene (NR) [1664 cm^{-1} (for $\nu_{C=C-}$), 1375 and 1448 cm^{-1} (for δ_{CH2} deformation), 837 cm^{-1}(for $\gamma_{=C-H}$ bending)].[20] Particularly, a new peak at 1539 cm^{-1} can be seen. According to the comparative analysis of FTIR spectra in Figure 2(b), this peak only exists in the vulcanized NR. It is revealed that this absorption peak is derived from the vulcanization process. This band was also observed by Joly et al. in their FTIR investigation of vulcanized NR.[21] Moreover, it is seen that the FTIR spectra are highly sensitive to the molecular structural changes during thermal oxidation aging. The absorption bands in the range of 1700–1850 cm^{-1} show the variation of carbonyl compound concentration [Fig. 2(c)].[22] For instance, the absorbencies of bands at 1728 and 1740 cm^{-1} increase during aging and a new peak at 1784 cm^{-1} appears, indicating the degradation of the vulcanized NR and appearance of low molecular weight products.[22] According to the literature, the absorption bands at 837 and 1728 cm^{-1} can be used to monitor the concentration change of double bond and carbonyl groups.[22] So, the intensities of the 837 and 1728 cm^{-1} bands as a function of time are shown in Figure 3. Meanwhile, the intensity variation of 1539 cm^{-1} band is also shown in Figure 3. Obviously, the intensity of 1539 cm^{-1} band changes significantly. So, it is suggested that 1539 cm^{-1} band is more sensitive to the thermal oxidation degradation process.

Figure 4 presents the SEM observations of the NR before and after three days' cyclic loading at 85°C. As to the sample not subject to high temperature fatigue loading, the fracture surface is smooth, with some zinc oxides homogeneously interspersed on it [Fig. 4(a)]. Figure 4(b) shows the SEM image of vulcanized NR after three days high temperature fatigue loading. Apparently, the fracture surface is rough and many tenuous nanoscale cracks can be seen. Meanwhile, decohesion between zinc oxides and rubber matrix does not occur. Three typical cracks were pointed by the yellow arrows. Besides, we can also see some nanoscale voids with a diameter of about several hundred nanometers [Fig. 4(c,d)]. Particularly, there are several nanoscale cracks (< 500 nm) exist in the neighborhood of the voids (pointed by the yellow arrows). After eight days high temperature fatigue loading, the surface is accidental and much more voids appear with diameters varying between a few hundred nanometers and several micrometers (Fig. 5). However, nanoscale cracks can hardly be seen.

For fatigue loading at room temperature, previous studies confirmed that micro-voids occur in the vicinity of the micro-crack tip because of the decohesion between zinc oxides and rubber matrix.[10,23] Here, we also tested the NR samples at the same condition with high temperature fatigue testing but under room temperature. The SEM images are shown in Figure 6. Figure 6(a) shows the vulcanized NR subject to three days fatigue loading under room temperature. It is seen that the surface is rather rough, but no nanoscale cracks or voids can be seen. As the NR sample was subject to eight days room temperature fatigue loading [Fig. 6(b)], the decohesion between zinc oxides and rubber matrix can be seen clearly. Comparing the high temperature and room temperature testing results, it can be concluded that the nanoscale cracks initiated during high temperature fatigue measurement arise from the combined impact of thermal oxidation and cyclic loading. Meanwhile, it can be deduced that the nanoscale voids initiated during high temperature fatigue measurement does not originate from the decohesion between zinc oxides and rubber matrix. It has been observed, that much more voids appear and nanoscale cracks can hardly be seen after eight days high temperature fatigue loading. Moreover,

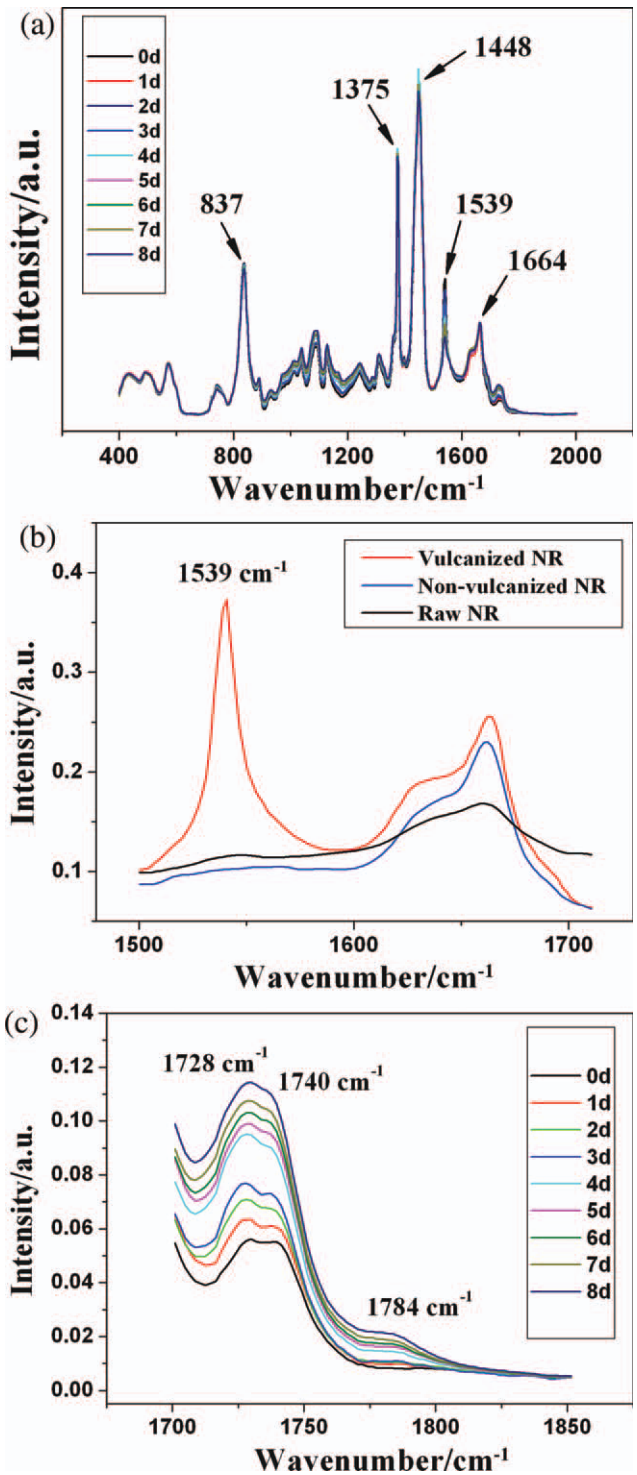

Figure 2 (a) Time-resolved IR spectra in the range 400–2000 cm^{-1} of vulcanized NR during aging. (b) IR spectra of raw NR, non-vulcanized NR (containing all the vulcanization ingredients) and vulcanized NR in the range of 1500–1710 cm^{-1}. (c) Panel c illustrates the intensity change of the IR spectra in the range of 1700–1785 cm^{-1}. [Color figure can be viewed in the online issue, which is available at wileyonlinelibrary.com.]

Figure 4(c,d) shows that the voids exist in the vicinity of the micro-crack tip (pointed by the yellow arrows). Thus, we propose that the voids may be originated from the evolution of the nanoscale cracks.

To study the mechanism of crack generation, the PALS measurements were employed to assess the crack initiation mechanism. Figure 7(a) shows the o-Ps lifetime variation of the vulcanized NR. It can be seen that τ_3 tends to increase from 2.45 to 2.57 ns. It decreases slightly only at the second day. The slight decrease may be experimental error and it can be neglected. This result indicates that the dimension of the free volume holes tends on the whole to increase when NR is subject to high temperature fatigue. To prove this, a semiempirical relationship between o-Ps lifetime and the average radius of the free volume holes is used:[24,25]

$$\tau_3 = \frac{1}{\lambda_3} = \frac{1}{2}\left[1 - \frac{R}{R_0} + \frac{1}{2\pi}\sin\left(\frac{2\pi R}{R_0}\right)\right]^{-1} \quad (1)$$

where R denotes the average radius of the free volume holes expressed in angstroms. R_o is equal to $R+\Delta R$, and ΔR=1.656 Å is the estimated empirical electron layer thickness. According to the calculated R from eq. (1), the average volume of the free volume holes can be obtained by using the spherical-hole model, i.e., $V_h = 4\pi R^3/3$. Figure 7(b) shows the variation of V_h during high temperature fatigue loading. Clearly, the V_h shows the same trend as that of τ_3.

The free volume fraction can be estimated according to the following empirical formula:

$$f_v = AV_hI_3 \quad (2)$$

where A is an empirical parameter determined to be 0.0018 from specific volume data by Wang et al.[26] I_3 is the o-Ps intensity which has been shown in Figure 7(c). The calculated f_v is exhibited in Figure 7(d).

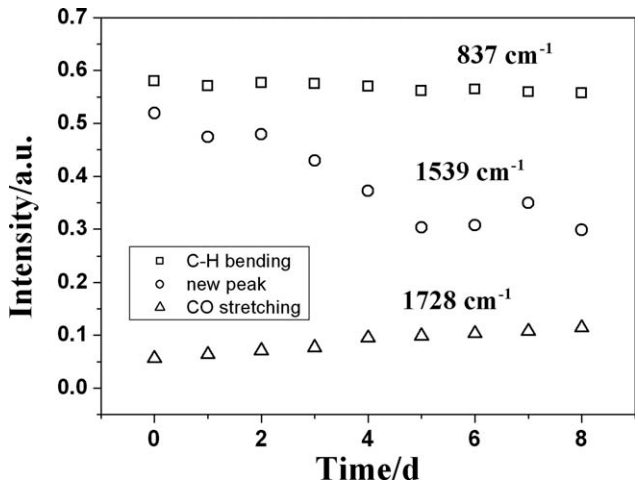

Figure 3 The intensity change of the characteristic absorption peaks at 837, 1728, and 1539 cm^{-1}.

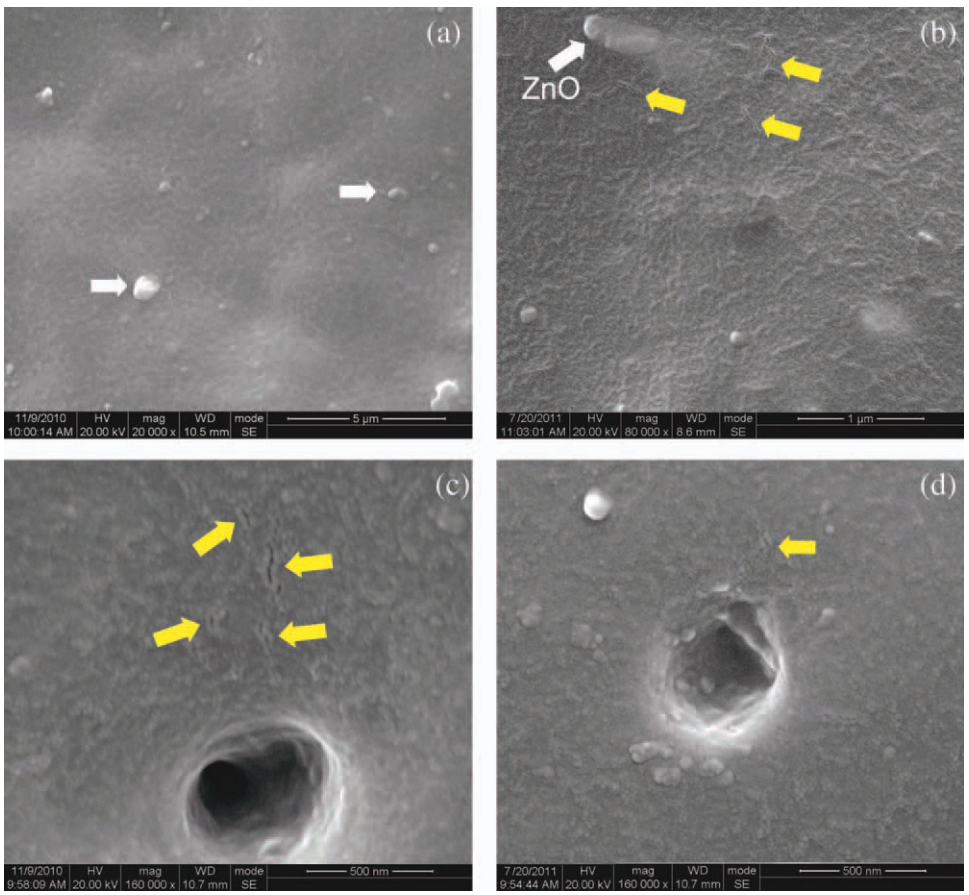

Figure 4 SEM observations of the NR samples before (a) and after three days' cyclic loading (b) at a temperature of 85°C. The white arrows denote the ZnO particles and the yellow arrows indicate the existence of nanoscale cracks. Panels (c) and (d) shows the existence of nanoscale voids. The nanoscale cracks (<500 nm) exist in the neighborhood of the voids. [Color figure can be viewed in the online issue, which is available at wileyonlinelibrary.com.]

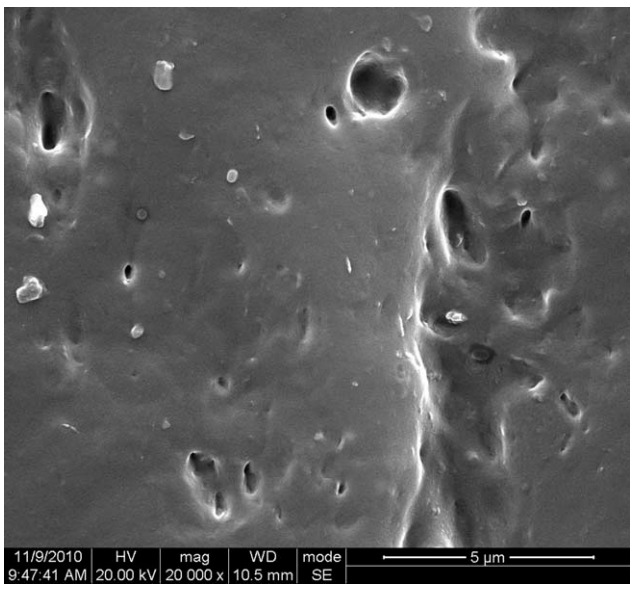

Figure 5 SEM image of NR after eight days' cyclic loading at a temperature of 85°C.

The free volume fraction maintains at the first two days and then it decrease significantly at the third day. Thereafter, f_v value gradually increases in the next three days and finally undergoes a slight decrease in the last two days. Consequently, the final f_v value is lower than that of the NR sample before fatigue loading.

Le Cam et al. deduced that cavitation takes place around zinc oxide particles and at the poles of metallic oxide inclusions.[10] Because of the influence of thermal oxidation, this conclusion cannot be applied to the present work, which has been proved above by the SEM measurements. Recently, Rozanski et al. investigated the initiation of cavitation of polypropylene during stretching.[17] They proposed that the presence of vapor or gas bubbles (namely, "empty" spaces) in the amorphous phase change in time as a result of thermal movements of the polymer chains. These "empty" spaces are conducive to the formation of cavities in the low molecular weight phase. In other words, the "empty" spaces are cavitation nuclei. This can be applicable to the present research.

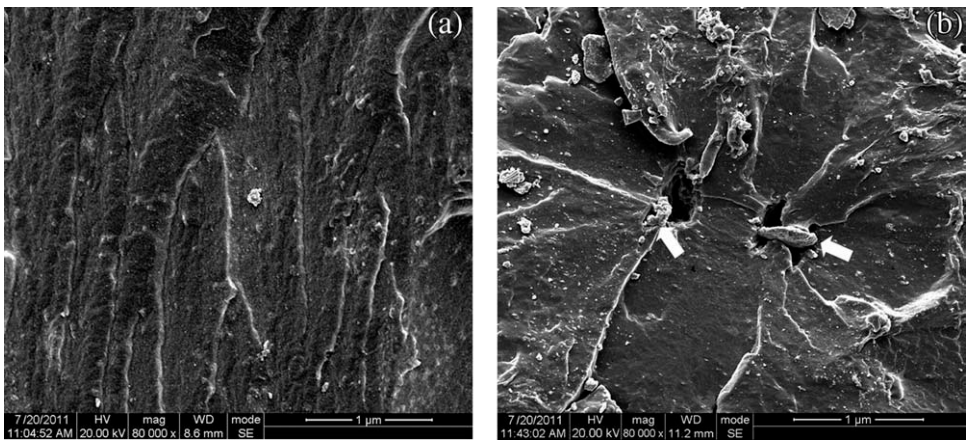

Figure 6 SEM images of NR after three day's cyclic loading (a) and eight days' cyclic loading (b) under room temperature.

As to the vulcanized NR, thermal degradation products with low molecular weight appear in the matrix. Meanwhile, NR contains 6 wt % natural impurities, including proteins (2.2 wt %), phospholipids and fatty acids (3.4%), carbohydrates (0.4%), and others (0.3 wt %).[27,28] At high temperature (85°C), some components can melt (e.g., fatty acids and carbohydrates). So, these two factors lead to the existence of low molecular weight domains in the NR matrix, which are conducive to the dissolution of vapor and gas ("empty" space). As the V_h value increases during the high temperature fatigue loading, vapor, and gas molecular diffusion is intensified, and it leads to easier concentration of dissolved vapor and gas in the low molecular weight domains, contributing to the formation of bigger vapor and gas bubbles. Dissolved vapor and gas thus become crack nuclei in the low molecular weight domains, leading to the initiation of

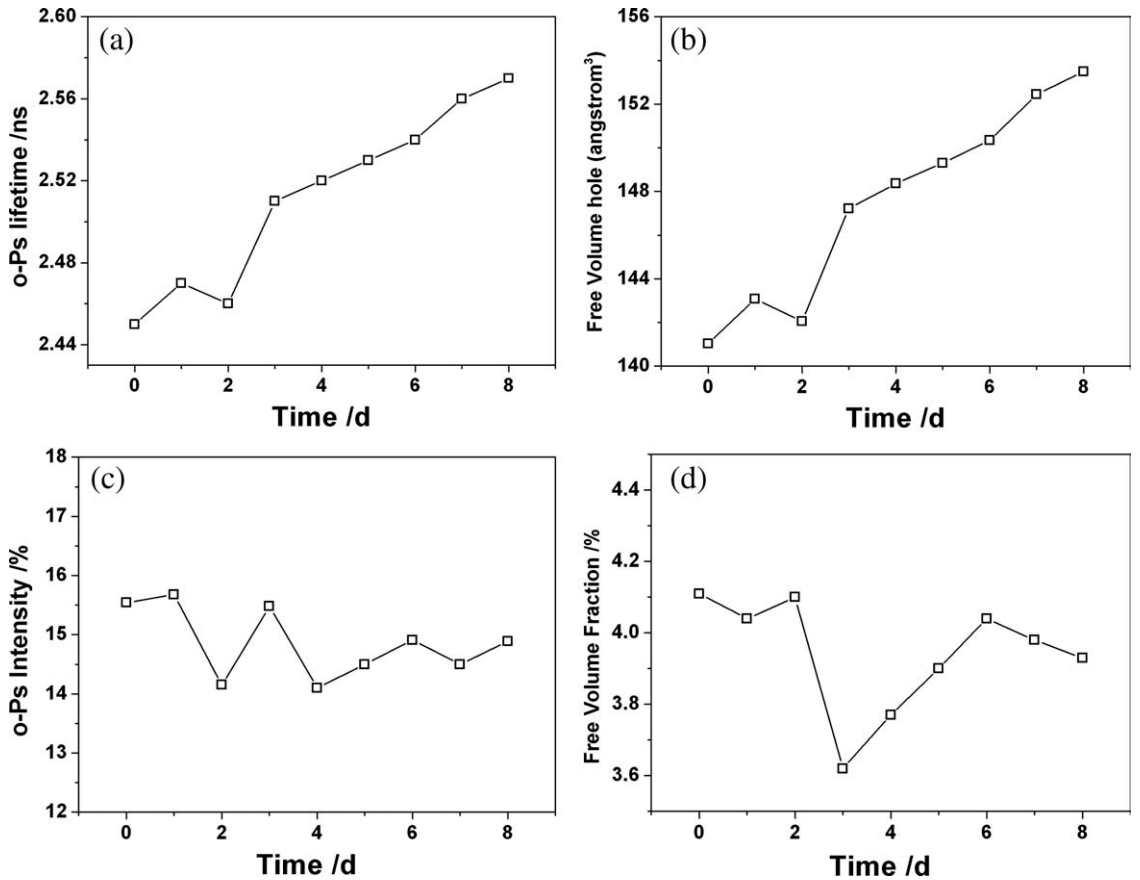

Figure 7 (a) PALS analysis results: high temperature fatigue time dependence of o-Ps lifetime of NR; (b) average volume variation of the free volume holes of NR during high temperature fatigue; (c) o-Ps intensity variation of NR during high temperature fatigue; (d) free volume fraction change of NR during high temperature fatigue.

nanoscale cracks under dynamic loading. As the nanoscale cracks further evolve during the present fatigue loading, nanoscale voids appear (see Fig. 4). Further, more nanoscale cracks evolve into nano- or micro-voids during fatigue (Fig. 5). Since, the volume of the NR sample irradiated by positron beam does not change and free volume holes in the cracks and voids areas disappear, the decrease of free volume fraction at the third day is observed [Fig. 7(d)]. The free volume fraction increase in the next three days implies the size and number increase of the free volume in NR matrix in the later fatigue process. As nanoscale cracks can hardly be seen in the later process of high temperature cyclic loading, we deduce the crack growth is significantly accelerated. In other words, as the nanoscale cracks are initiated, they evolve into voids very fast.

CONCLUSIONS

During thermal oxidation aging, mechanical properties of NR deteriorate gradually. Thermal oxidation degradation of the vulcanized NR is investigated by FTIR analysis. The vulcanized NR was simultaneously subject to high temperature (85°C) and cyclic loading. Under these conditions, SEM images confirmed the appearance of nanoscale cracks and voids which are initiated by the combined impact of high temperature and cyclic loading. Further, PALS measurements monitored the free volume size and content changes of the NR during high temperature fatigue. Unlike the condition of fatigue loading at room temperature, crack generation is derived from the nucleation effect of the dissolved vapor and gas in the low molecular weight domains of the NR. Thermal degradation products account for the appearance of the low molecular weight domains. As the cracks evolve, nano-scale voids appear. Further evolution of the smaller voids leads to the larger spherical voids with their diameters varying between a few hundred nanometers and several microns.

References

1. Mars, W. V.; Fatemi, A. Int J Fatigue 2002, 112, 151.
2. Menon, A. R. R.; Pillai, C. K. S.; Jin, W. S.; Nah, C. Polym Int 2005, 54, 629.
3. Rivlin, R. S.; Thomas, A. G. J Polym Sci 1953, 10, 291.
4. Aglin, H.; Moet, A. Int J Fract 1989, 40, 285.
5. Thomas, A. G. Rubber Chem Technol 1994, 67, G50.
6. Bathias, C.; Legorju-jago, K. Int J Fatigue 2002, 24, 85.
7. Batemann, L. The Chemistry and Physics of Rubber-Like Substance; Maclaren & Sons: London, 1963.
8. Roberts, A. D. Natural Rubber Science and Technology; Oxford University Press: Oxford, 1988.
9. Mark, J. E.; Erman, B. Rubber Elasticity: A Molecular Primer; Wiley Interscience: New York, 1988.
10. Le Cam, J. B.; Huneau, B.; Verron, E.; Gornet, L. Macromolecules 2004, 37, 5011.
11. Medalia, A. I. Rubber Chem Technol 1991, 64, 481.
12. Kakavas, P. A. J Appl Polym Sci 1996, 59, 251.
13. Weng, G. S.; Huang, G. S.; Qu, L. L.; Zhang, P.; Nie, Y. J.; Wu, J. R. J Appl Polym Sci 2010, 118, 2050.
14. Vallery, R. S.; Liu, M.; Gidley, D. W.; Launey, M. E.; Kruzic, J. J. Appl Phys Lett 2007, 91, 261908.
15. Launey, M. E.; Busch, R.; Kruzic, J. J. Scr Mater 2006, 54, 483.
16. Launey, M. E.; Busch, R.; Kruzic, J. J. Acta Mater 2008, 56, 500.
17. Rozanski, A.; Galeski, A.; Debowska, M. Macromolecules 2011, 44, 20.
18. Weng, G. S.; Huang, G. S.; Qu, L. L.; Nie, Y. J.; Wu, J. R. J Phys Chem B 2010, 114, 7179.
19. Cai, H. H.; Li, S. D.; Tian, G. R.; Wang, H. B.; Wang, J. H. J Appl Polym Sci 2003, 87, 982.
20. Tripathy, A. R.; Morin, J. E.; Williams, D. E.; Eyles, S. J.; Farris, R. J. Macromolecules 2002, 35, 4616.
21. Joly, S.; Garnaud, G.; Ollitrault, R.; Bokobza, L.; Mark, J. E. Chem Mater 2002, 14, 4202.
22. Colin, X.; Audouin, L.; Verdu, J. Polym Degrad Stab 2007, 92, 886.
23. Layouni, K.; Laiarinandrasana, L.; Piques, R. In Consititutive Models for Rubber, 3rd ed.; Busfiled, J., Muhr, A., Eds.; A. A. Balkema: Lisse, 2003; p 273.
24. Tao, S. J. J Chem Phys 1972, 56, 6268.
25. Eldrup, M.; Lightbody, D.; Sherwood, J. N. Chem Phys 1981, 63, 51.
26. Wang, Y. Y.; Nakanishi, H.; Jean, Y. C.; Sandreczki, T. C. J Polym Sci Part B: Polym Phys 1990, 28, 1431.
27. Karino, T.; Ikeda, Y.; Yasuda, Y.; Kohjiya, S.; Shibayama, M. Biomacromolecules 2007, 8, 693.
28. Kohjiya, S.; Tosaka, M.; Furutani, M.; Ikeda, Y.; Toki, S.; Hsiao, B. S. Polymer 2007, 48, 3801.